

Research Article

Selection of Oxide Materials for Use in a Thermal Barrier Coating System

Adalat S. Samadov¹, Tural B. Usubaliyev², Parviz Sh. Abdullayev³, Ibrahim A. Muradzade⁴

^{1,2,3,4}*Flight Equipment and Aviation Engines Department, National Aviation Academy, Baku, Azerbaijan.*

²*Corresponding Author : tural.u@innovations.com.tr*

Received: 01 January 2025

Revised: 03 February 2025

Accepted: 21 February 2025

Published: 05 March 2025

Abstract - Since the lifetime of hot-section components directly affects the main characteristics of the Gas Turbine Engine (GTE), their thermal protection is carried out by Thermal Barrier Coatings (TBC). Although this coating system consists of several layers, the main layer that provides thermal insulation is the top layer. One of the main reasons for the long-term operation of this type of coating in aggressive environments is the presence of oxide material in its composition. To meet the requirements of this environment, oxides are the focus of the search for new and alternative TBC materials. These materials are currently in an active development phase. Their thermo-mechanical properties usually determine the effectiveness of oxide materials. Therefore, much attention is paid to their properties when selecting oxide materials for the top layer. In this paper, the optimal TBC material was selected by taking into account the properties of a large number of oxide materials. The study was conducted using the Analytical Network Process (ANP) methodology. Ultimately, these results demonstrate that $Gd_2Zr_2O_7$ has the highest rank among all the studied materials and is the most promising candidate for the top layer.

Keywords - Gas turbine engines, Thermal barrier coating materials, Thermal and mechanical properties, Analytic network process.

1. Introduction

The operational reliability of the engines is determined by the observance and implementation of the established operating modes, as well as by maintaining the stability of the structure and properties of materials during the entire lifetime. The ever-increasing operating temperature and acting stresses require an increase in materials' physical, mechanical and operational properties and their preservation throughout the lifetime. These properties are largely determined by thermal structural stability, heat, and corrosion resistance [1, 2]. Therefore, studying the relationship between the chemical composition and the specified properties is an objective and especially important for newly developed alloys, considering the specifics of their application. The only way that the turbines can survive in such an extremely harsh environment is by effective cooling systems, which, nevertheless, negatively affect the overall efficiency of the gas turbine engines (GTEs). To address these problems, an alternative concept has been introduced and developed over the past decades, using advanced thermal barrier coatings (TBCs) on superalloys [3-13].

The performance characteristics of hot section components, which are one of the main sections of the GTEs, largely depend on the correct choice of TBCs. The coatings protect engine hot section components by acting as a thermal

insulator layer between the base metal (with cooling system) and the hot gases to which they are exposed. Also, the correct choice of TBCs, applied to the components in a GTE, provided component temperature reductions of up to 300°C, depending on the thickness [12-17].

The achievement of the required level of performance of the GTE's hot section components is associated with creating an efficient system, "superalloy-TBC". Modern high-temperature Ni-based superalloys used in GTE blades possess the required level of long-term strength due to their low corrosion resistance to combustion products, but they do not meet the requirements for blade lifetime. To ensure the required durability of the TBCs, along with the correct choice of the chemical composition, the processes occurring at the boundary of the substrate and the coating should be taken into account, which directly affect their operational reliability.

The fact is that this coating differs from the others in that it consists of multilayers, and each one has its specific function and properties. This type of coating is the most complex among all coatings and is made of different materials. The complexity is that these types of coatings are heterogeneities in properties (physical, thermal, chemical and mechanical) of each layer [13].



This paper will not discuss any other layer materials of the TBC system except the top layer. Various oxide materials are considered suitable for use as a top coat layer. However, given the many requirements that TBC must meet, choosing the best material is never easy. The materials intended for the top layer in the TBC coating should possess a range of properties and requirements to withstand high thermal and mechanical loads, which include high temperature resistance, low thermal conductivity, high fracture toughness, and an appropriate thermal expansion coefficient high melting point, good adhesion to the metal substrate, high thermal stability, strain tolerance, high chemical stability, low sintering rate,

high corrosion resistance and low density [3, 18, 19]. Satisfying several requirements simultaneously complicates selecting the best candidate among the possible materials and makes it a multi-criteria task. Moreover, the large number of candidates, in turn, makes this task even more difficult. Therefore, various approaches have been proposed to solve this problem, making it easier and less tedious. This paper examines the possibility of selecting the best candidate material using one of the approaches proposed by Ashby [20], based on the principle of the Analytical Network Process (ANP) [21]. This study will be carried out in the following main stages (see Fig. 1).



Fig. 1 Workflow chart

2. Materials and Methods

2.1. Materials

In this study, a database of materials collected from various references were created, which includes the following materials: SrZrO_3 [22, 23], Yb_3NbO_7 [24], Yb_3TaO_7 [24], $\text{LaTi}_2\text{Al}_9\text{O}_{19}$ [25], $\text{La}_2\text{Zr}_2\text{O}_7$ [26-28], Mg_2SiO_4 [29], $\text{La}_2\text{Hf}_2\text{O}_7$ [30], $\text{La}_2\text{Ce}_2\text{O}_7$ [31, 32] and $\text{Gd}_2\text{Zr}_2\text{O}_7$ [33]. Important properties were selected for these materials, including specific heat capacity, thermal diffusivity, thermal conductivity, thermal expansion coefficient, Young's modulus, hardness, and fracture toughness. Each property has a different impact on the performance of the entire coating, and these impacts are designated as positive and negative. This is done because this method considers the highest value to be the best, and by marking certain properties as negative, the line of reasoning is reversed, and the lowest value is considered the best. Let us consider this using the example of thermal conductivity. Low thermal conductivity materials absorb heat from the environment slowly and transport heat poorly, while high thermal conductivity materials may transfer heat efficiently. If a thermal barrier is required on the surface of the substrate and the temperature is reduced, materials with low thermal conductivity are needed to solve this problem, and this property is noted as negative. Conversely, if the task were to ensure good heat transfer to the air (heating and cooling), materials with high thermal conductivity would be chosen, and this property would be noted as positive. The remaining properties are specified similarly. Table 1 shows the values and effects of selected properties.

2.2. Methodology

The materials in the current study are ranked according to various parameters regarding their suitability as TBCs using an ANP. ANP proposed by Saaty can be considered a powerful tool for solving multi-attribute decision-making problems [21]. ANP can be considered an extension of the Analytic Hierarchy Process, offering feedback and interaction

inside and across sets of alternatives and criteria. This implies that elements within a cluster might impact one another (i.e., inner dependence) and that alternatives within a cluster may depend on certain criteria situated in another cluster (i.e., outer dependence). Moreover, these inner and outer dependencies make it possible to consider all possible influences between clusters and select the best candidate material.

This method consists of several main steps. These steps are shown in Figure 2 and discussed in detail in this section.

The model must be built in the first step, and the problem must be structured. The problem must be clearly stated and divided into a rational system, such as a network. A schematic representation of the feedback between alternatives and criteria to be used in this work will be presented in Figure 3.

The ANP solution procedure is based on pairwise comparisons of elements of a given solution space, based on which it is possible to compare values in clusters and understand how much one value is greater than another, (for example, f_3 in relation to f_5 in cluster A_7 is better or worse by f_3/f_5 times). This method allows for comparing any quantities, regardless of whether they are in the same or different units of measurement, which makes it universal in this regard. However, before answering these questions, you need to obtain a pairwise comparison matrix as shown in the sequential order below. Each material is unique because it has characteristics that set it apart from other materials. These properties can have a direct and indirect impact on the performance characteristics of the material itself. Depending on the level of impact of a property, the decision maker can designate primary and secondary properties in the ANP method. The properties are divided into clusters, and weights are assigned to them, indicating their degree of influence or importance. In this case, as shown in Figure 4, the properties are divided into thermal and mechanical clusters.

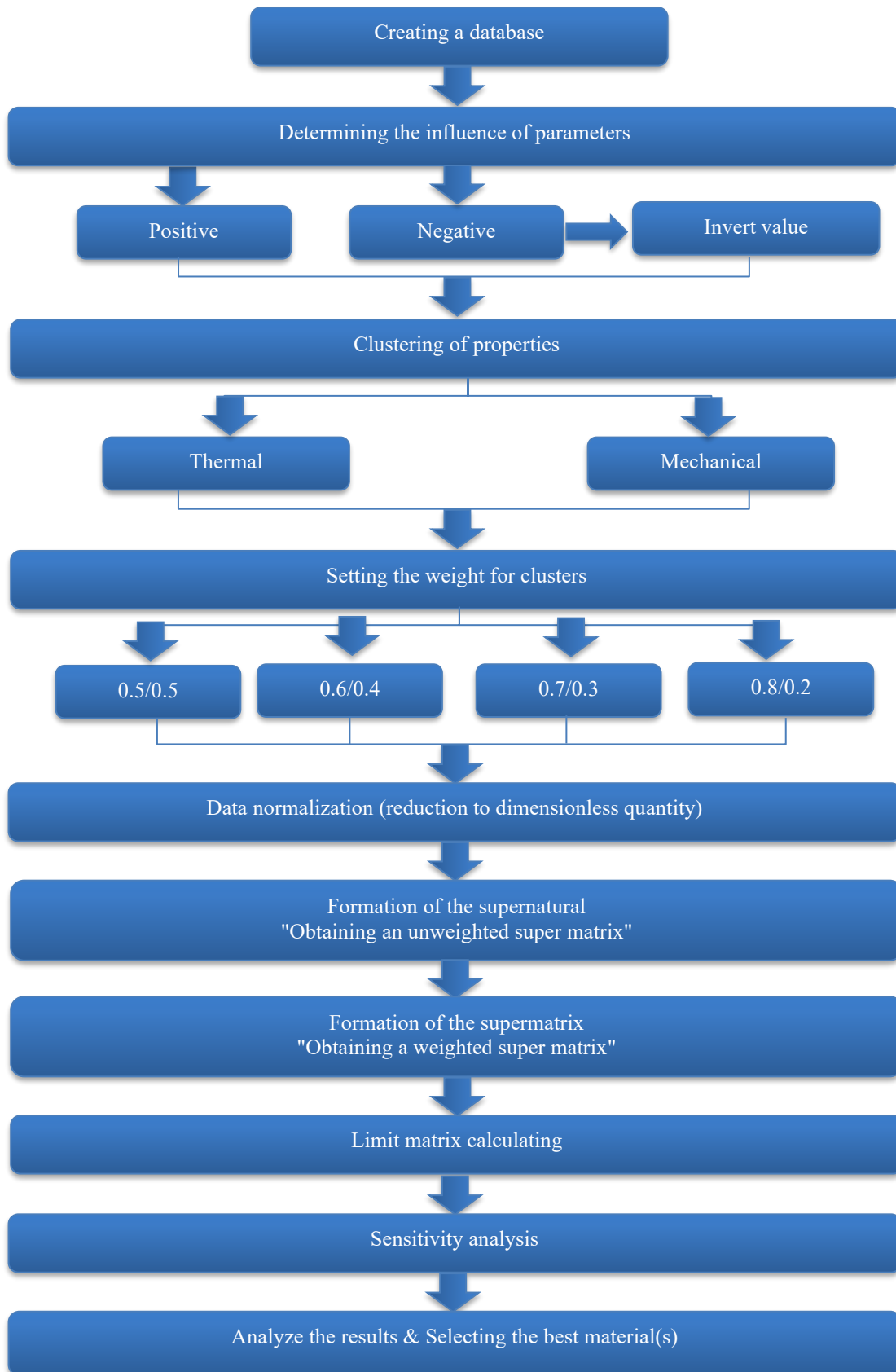


Fig. 2 The main steps of the Selection process

Table 1. Material parameters

			SrZrO ₃	Yb ₃ NbO ₇	Yb ₃ TaO ₇	LaTi ₂ Al ₉ O ₁₉	La ₂ Zr ₂ O ₇	Mg ₂ SiO ₄	La ₂ Hf ₂ O ₇	La ₂ Ce ₂ O ₇	Gd ₂ Zr ₂ O ₇	Effect on performance
Properties	Unit	Index	A_1	A_2	A_3	A_4	A_5	A_6	A_7	A_8	A_9	
Specific heat capacity (C_p)	J/kg·K	f_1	0.560	0.395	0.354	0.958	0.480	0.160	0.287	0.429	0.440	Negative
Thermal diffusivity (D_{th})	m ² ·s ⁻¹ (×10 ⁻⁶)	f_2	0.824	0.316	0.350	0.385	0.675	0.915	0.858	0.344	0.299	Negative
Thermal conductivity (λ)	W·m ⁻¹ ·K ⁻¹	f_3	2.423	1.100	1.244	1.215	1.694	2.405	2.204	0.895	0.919	Negative
Thermal expansion coefficient (α)	K ⁻¹ (×10 ⁻⁶)	f_4	9.923	9.698	9.214	9.733	8.602	9.977	8.759	11.709	10.300	Positive
Young's modulus (E)	GPa	f_5	170.0	208.9	191.9	240.0	175.0	185.0	216.4	91.0	249.6	Negative
Hardness (H_V)	GPa	f_6	9.20	8.00	9.80	7.10	9.90	10.00	9.81	6.10	16.60	Positive
Fracture toughness (K_{IC})	MPa·m ^{1/2}	f_7	1.50	1.50	1.70	1.30	1.10	2.80	2.27	1.10	1.50	Positive

Note: specific heat capacity, thermal diffusivity, thermal conductivity, and coefficient of thermal expansion values shown are average values over the temperature range tested.

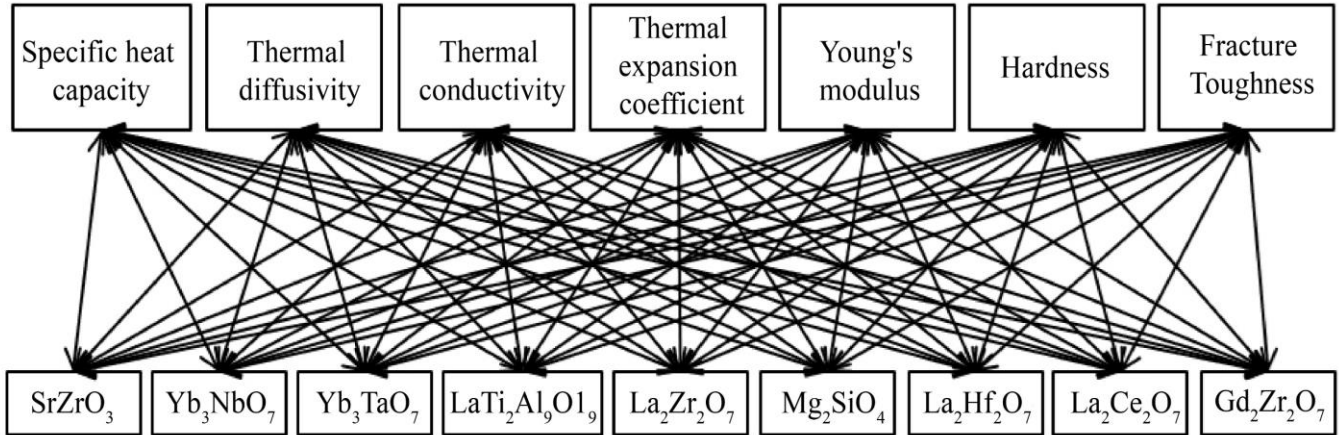


Fig. 3 ANP structure in an example of choosing the best TBC candidate material

Cluster 1 Thermal properties	Cluster 2 Mechanical properties
Specific heat capacity	Young's modulus
Thermal diffusivity	Hardness
Thermal conductivity	Fracture toughness
Thermal expansion coefficient	

Fig. 4 Cluster of properties

In order to compare materials and their properties, it is necessary to bring them into a single form, i.e. normalize. Normalization is converting values with various measuring units to a single dimensionless form. To normalize an entry, dividing it by the total of all the entries in a specific row is necessary. For the case where attribute values have a negative

effect, you must first invert the values and then normalize the resulting inverted values. As a result, the normalized matrix presented in Table 2 is obtained.

This normalized priority matrix will then be collected into an unweighted super matrix for further calculations because the unweighted super matrix is formed from the normalized matrix. Based on the normalized matrix, each criterion in the clusters (thermal and mechanical) is assigned a preference number, i.e. its obtained values are ranked from best to worst (for example, for A_1 , f_1 has the second rank, f_2 has the fourth rank, f_3 has the third rank, f_4 has the first rank). An unweighted super matrix is obtained by inverting the ranks and normalizing the values (see Table 3). At the next stage, weights are assigned for each cluster.

Table 2. Normalized matrix

Properties	Index	SrZrO ₃	Yb ₃ NbO ₇	Yb ₃ TaO ₇	LaTi ₂ Al ₉ O ₁₉	La ₂ Zr ₂ O ₇	Mg ₂ SiO ₄	La ₂ Hf ₂ O ₇	La ₂ Ce ₂ O ₇	Gd ₂ Zr ₂ O ₇
		A_1	A_2	A_3	A_4	A_5	A_6	A_7	A_8	A_9
C_p	f_1	0.0726	0.1029	0.1148	0.0424	0.0847	0.2540	0.1416	0.0947	0.0924
D_{th}	f_2	0.0612	0.1596	0.1441	0.1310	0.0747	0.0551	0.0588	0.1466	0.1687
λ	f_3	0.0624	0.1374	0.1215	0.1244	0.0893	0.0629	0.0686	0.1689	0.1645
α	f_4	0.1129	0.1103	0.1048	0.1107	0.0978	0.1135	0.0996	0.1332	0.1172
E	f_5	0.1158	0.0943	0.1026	0.0820	0.1125	0.1064	0.0910	0.2164	0.0789
H_V	f_6	0.1063	0.0925	0.1133	0.0821	0.1144	0.1156	0.1134	0.0705	0.1919
K_{IC}	f_7	0.1016	0.1016	0.1151	0.0880	0.0745	0.1896	0.1537	0.0745	0.1016

Table 3. Unweighted super matrix

Properties		f_1	f_2	f_3	f_4	f_5	f_6	f_7	A_1	A_2	A_3	A_4	A_5	A_6	A_7	A_8	A_9
C_p	f_1	0	0	0	0	0	0	0	0.240	0.120	0.160	0.120	0.160	0.480	0.480	0.120	0.120
D_{th}	f_2	0	0	0	0	0	0	0	0.120	0.480	0.480	0.480	0.120	0.120	0.120	0.240	0.480
λ	f_3	0	0	0	0	0	0	0	0.160	0.240	0.240	0.240	0.240	0.160	0.160	0.480	0.240
α	f_4	0	0	0	0	0	0	0	0.480	0.160	0.120	0.160	0.480	0.240	0.240	0.160	0.160
E	f_5	0	0	0	0	0	0	0	0.545	0.273	0.182	0.182	0.273	0.182	0.182	0.545	0.182
H_V	f_6	0	0	0	0	0	0	0	0.273	0.182	0.273	0.273	0.545	0.273	0.273	0.182	0.545
K_{IC}	f_7	0	0	0	0	0	0	0	0.182	0.545	0.545	0.545	0.182	0.545	0.545	0.273	0.273
SrZrO ₃	A_1	0.073	0.061	0.062	0.113	0.116	0.106	0.102	0	0	0	0	0	0	0	0	0
Yb ₃ NbO ₇	A_2	0.103	0.160	0.137	0.110	0.094	0.092	0.102	0	0	0	0	0	0	0	0	0
Yb ₃ TaO ₇	A_3	0.115	0.144	0.122	0.105	0.103	0.113	0.115	0	0	0	0	0	0	0	0	0
LaTi ₂ Al ₉ O ₁₉	A_4	0.042	0.131	0.124	0.111	0.082	0.082	0.088	0	0	0	0	0	0	0	0	0
La ₂ Zr ₂ O ₇	A_5	0.085	0.075	0.089	0.098	0.113	0.114	0.074	0	0	0	0	0	0	0	0	0
Mg ₂ SiO ₄	A_6	0.254	0.055	0.063	0.113	0.106	0.116	0.190	0	0	0	0	0	0	0	0	0
La ₂ Hf ₂ O ₇	A_7	0.142	0.059	0.069	0.100	0.091	0.113	0.154	0	0	0	0	0	0	0	0	0
La ₂ Ce ₂ O ₇	A_8	0.095	0.147	0.169	0.133	0.216	0.071	0.074	0	0	0	0	0	0	0	0	0
Gd ₂ Zr ₂ O ₇	A_9	0.092	0.169	0.165	0.117	0.079	0.192	0.102	0	0	0	0	0	0	0	0	0

As mentioned earlier, the decision maker can set weights for each cluster, and the following sets of weights were selected in this study: (1) thermal cluster – 50%, mechanical cluster – 50%; (2) thermal cluster – 60%, mechanical cluster – 40%; (3) thermal cluster – 70%, mechanical cluster – 30%; and (4) thermal cluster – 80%, mechanical cluster – 20%. After setting the weights, each property entry was multiplied by the weight of the corresponding cluster (see Tables 4-7). The limit matrix is a mathematical concept used to obtain the (final) global weights of all solution elements in the solution space. The limit matrix is obtained by multiplying the weighted super matrix until all row values in the matrix are the same. The material with the highest global score is considered the best. The obtained limit matrices for different sets of weights are shown in Tables 8-11.

3. Results and Discussion

ANP is a powerful tool for solving multi-attribute decision-making problems, offering feedback and interaction inside and across sets of alternatives and criteria. Due to these dependencies, parameters can be easily compared, and the best candidate can be selected. For example, how does La₂Zr₂O₇ differ from SrZrO₃ regarding its thermal expansion coefficient? This can be done by referring to Table 2 and comparing the corresponding values, i.e. 0.1305/0.1506 =

0.867. In the same way, the properties of a specific material can be compared. For example, how important is the thermal conductivity property of La₂Ce₂O₇ compared to its thermal expansion coefficient? Thus, more information can be obtained through feedback, which allows for a comprehensive definition of the solution to the problem.

First, a normalized decision matrix was obtained based on the data presented in Table 1 (Table 2). Then, two classifications (clusters) of properties were used – thermal/mechanical and their weight ratios were adopted with the following ratios: (1) 0.5/0.5, (2) 0.6/0.4, (3) 0.7/0.3 and (4) 0.8/0.2. Next, after denoting the weights, weighted super matrices were obtained for the three sets by multiplying the weights by the corresponding clusters, as shown in Tables 4-7. The final step is to find the limit matrix, which was done by multiplying the weighted super matrix until all row values are the same, as presented in Tables 8-11. Finally, based on the obtained global weight, the candidate materials are ranked and the results are shown in Table 12. Thus, based on the results obtained, the following conclusions can be drawn:

1) Gd₂Zr₂O₇ showed the best values among the others, regardless of the set of cluster weights, and takes an honorable first place. Therefore, this material can be considered the best material.

Table 4. Weighted super matrix – thermal (50%) and mechanical (50%)

Properties		f_1	f_2	f_3	f_4	f_5	f_6	f_7	A_1	A_2	A_3	A_4	A_5	A_6	A_7	A_8	A_9
C_p	f_1	0	0	0	0	0	0	0	0.120	0.060	0.080	0.060	0.080	0.240	0.240	0.06	0.060
D_{th}	f_2	0	0	0	0	0	0	0	0.060	0.240	0.240	0.240	0.060	0.060	0.060	0.12	0.240
λ	f_3	0	0	0	0	0	0	0	0.080	0.120	0.120	0.120	0.120	0.080	0.080	0.24	0.120
α	f_4	0	0	0	0	0	0	0	0.240	0.080	0.060	0.080	0.240	0.120	0.120	0.08	0.080
E	f_5	0	0	0	0	0	0	0	0.273	0.136	0.091	0.091	0.136	0.091	0.091	0.273	0.091
H_V	f_6	0	0	0	0	0	0	0	0.136	0.091	0.136	0.136	0.273	0.136	0.136	0.091	0.273
K_{IC}	f_7	0	0	0	0	0	0	0	0.091	0.273	0.273	0.273	0.091	0.273	0.273	0.136	0.136
$SrZrO_3$	A_1	0.073	0.061	0.062	0.113	0.116	0.106	0.102	0	0	0	0	0	0	0	0	0
Yb_3NbO_7	A_2	0.103	0.160	0.137	0.110	0.094	0.092	0.102	0	0	0	0	0	0	0	0	0
Yb_3TaO_7	A_3	0.115	0.144	0.122	0.105	0.103	0.113	0.115	0	0	0	0	0	0	0	0	0
$LaTi_2Al_9O_{19}$	A_4	0.042	0.131	0.124	0.111	0.082	0.082	0.088	0	0	0	0	0	0	0	0	0
$La_2Zr_2O_7$	A_5	0.085	0.075	0.089	0.098	0.113	0.114	0.074	0	0	0	0	0	0	0	0	0
Mg_2SiO_4	A_6	0.254	0.055	0.063	0.113	0.106	0.116	0.190	0	0	0	0	0	0	0	0	0
$La_2Hf_2O_7$	A_7	0.142	0.059	0.069	0.100	0.091	0.113	0.154	0	0	0	0	0	0	0	0	0
$La_2Ce_2O_7$	A_8	0.095	0.147	0.169	0.133	0.216	0.071	0.074	0	0	0	0	0	0	0	0	0
$Gd_2Zr_2O_7$	A_9	0.092	0.169	0.165	0.117	0.079	0.192	0.102	0	0	0	0	0	0	0	0	0

Table 5. Weighted super matrix – thermal (60%) and mechanical (40%)

Properties		f_1	f_2	f_3	f_4	f_5	f_6	f_7	A_1	A_2	A_3	A_4	A_5	A_6	A_7	A_8	A_9
C_p	f_1	0	0	0	0	0	0	0	0.144	0.072	0.096	0.072	0.096	0.288	0.288	0.072	0.072
D_{th}	f_2	0	0	0	0	0	0	0	0.072	0.288	0.288	0.288	0.072	0.072	0.072	0.144	0.288
λ	f_3	0	0	0	0	0	0	0	0.096	0.144	0.144	0.144	0.144	0.096	0.096	0.288	0.144
α	f_4	0	0	0	0	0	0	0	0.288	0.096	0.072	0.096	0.288	0.144	0.144	0.096	0.096
E	f_5	0	0	0	0	0	0	0	0.218	0.109	0.073	0.073	0.109	0.073	0.073	0.218	0.073
H_V	f_6	0	0	0	0	0	0	0	0.109	0.073	0.109	0.109	0.218	0.109	0.109	0.073	0.218
K_{IC}	f_7	0	0	0	0	0	0	0	0.073	0.218	0.218	0.218	0.073	0.218	0.218	0.109	0.109
$SrZrO_3$	A_1	0.073	0.061	0.062	0.113	0.116	0.106	0.102	0	0	0	0	0	0	0	0	0
Yb_3NbO_7	A_2	0.103	0.160	0.137	0.110	0.094	0.092	0.102	0	0	0	0	0	0	0	0	0
Yb_3TaO_7	A_3	0.115	0.144	0.122	0.105	0.103	0.113	0.115	0	0	0	0	0	0	0	0	0
$LaTi_2Al_9O_{19}$	A_4	0.042	0.131	0.124	0.111	0.082	0.082	0.088	0	0	0	0	0	0	0	0	0
$La_2Zr_2O_7$	A_5	0.085	0.075	0.089	0.098	0.113	0.114	0.074	0	0	0	0	0	0	0	0	0
Mg_2SiO_4	A_6	0.254	0.055	0.063	0.113	0.106	0.116	0.190	0	0	0	0	0	0	0	0	0
$La_2Hf_2O_7$	A_7	0.142	0.059	0.069	0.100	0.091	0.113	0.154	0	0	0	0	0	0	0	0	0
$La_2Ce_2O_7$	A_8	0.095	0.147	0.169	0.133	0.216	0.071	0.074	0	0	0	0	0	0	0	0	0
$Gd_2Zr_2O_7$	A_9	0.092	0.169	0.165	0.117	0.079	0.192	0.102	0	0	0	0	0	0	0	0	0

Table 6. Weighted super matrix – thermal (70%) and mechanical (30%)

Properties		f_1	f_2	f_3	f_4	f_5	f_6	f_7	A_1	A_2	A_3	A_4	A_5	A_6	A_7	A_8	A_9
C_p	f_1	0	0	0	0	0	0	0	0.168	0.084	0.112	0.084	0.112	0.336	0.336	0.084	0.084
D_{th}	f_2	0	0	0	0	0	0	0	0.084	0.336	0.336	0.336	0.084	0.084	0.084	0.168	0.336
λ	f_3	0	0	0	0	0	0	0	0.112	0.168	0.168	0.168	0.168	0.112	0.112	0.336	0.168
α	f_4	0	0	0	0	0	0	0	0.336	0.112	0.084	0.112	0.336	0.168	0.168	0.112	0.112
E	f_5	0	0	0	0	0	0	0	0.164	0.082	0.055	0.055	0.082	0.055	0.055	0.164	0.055
H_V	f_6	0	0	0	0	0	0	0	0.082	0.055	0.082	0.082	0.164	0.082	0.082	0.055	0.164
K_{IC}	f_7	0	0	0	0	0	0	0	0.055	0.164	0.164	0.164	0.055	0.164	0.164	0.082	0.082
$SrZrO_3$	A_1	0.073	0.061	0.062	0.113	0.116	0.106	0.102	0	0	0	0	0	0	0	0	0
Yb_3NbO_7	A_2	0.103	0.160	0.137	0.110	0.094	0.092	0.102	0	0	0	0	0	0	0	0	0
Yb_3TaO_7	A_3	0.115	0.144	0.122	0.105	0.103	0.113	0.115	0	0	0	0	0	0	0	0	0
$LaTi_2Al_9O_{19}$	A_4	0.042	0.131	0.124	0.111	0.082	0.082	0.088	0	0	0	0	0	0	0	0	0
$La_2Zr_2O_7$	A_5	0.085	0.075	0.089	0.098	0.113	0.114	0.074	0	0	0	0	0	0	0	0	0
Mg_2SiO_4	A_6	0.254	0.055	0.063	0.113	0.106	0.116	0.190	0	0	0	0	0	0	0	0	0

$\text{La}_2\text{Hf}_2\text{O}_7$	A_7	0.142	0.059	0.069	0.100	0.091	0.113	0.154	0	0	0	0	0	0	0	0
$\text{La}_2\text{Ce}_2\text{O}_7$	A_8	0.095	0.147	0.169	0.133	0.216	0.071	0.074	0	0	0	0	0	0	0	0
$\text{Gd}_2\text{Zr}_2\text{O}_7$	A_9	0.092	0.169	0.165	0.117	0.079	0.192	0.102	0	0	0	0	0	0	0	0

Table 7. Weighted super matrix – thermal (80%) and mechanical (20%)

Properties		f_1	f_2	f_3	f_4	f_5	f_6	f_7	A_1	A_2	A_3	A_4	A_5	A_6	A_7	A_8	A_9
C_p	f_1	0	0	0	0	0	0	0	0.192	0.096	0.128	0.096	0.128	0.384	0.384	0.096	0.096
D_{th}	f_2	0	0	0	0	0	0	0	0.096	0.384	0.384	0.384	0.096	0.096	0.096	0.192	0.384
λ	f_3	0	0	0	0	0	0	0	0.128	0.192	0.192	0.192	0.192	0.128	0.128	0.384	0.192
α	f_4	0	0	0	0	0	0	0	0.384	0.128	0.096	0.128	0.384	0.192	0.192	0.128	0.128
E	f_5	0	0	0	0	0	0	0	0.109	0.055	0.036	0.036	0.055	0.036	0.036	0.109	0.036
H_V	f_6	0	0	0	0	0	0	0	0.055	0.036	0.055	0.055	0.109	0.055	0.055	0.036	0.109
K_{IC}	f_7	0	0	0	0	0	0	0	0.036	0.109	0.109	0.109	0.036	0.109	0.109	0.055	0.055
SrZrO_3	A_1	0.073	0.061	0.062	0.113	0.116	0.106	0.102	0	0	0	0	0	0	0	0	0
Yb_3NbO_7	A_2	0.103	0.160	0.137	0.110	0.094	0.092	0.102	0	0	0	0	0	0	0	0	0
Yb_3TaO_7	A_3	0.115	0.144	0.122	0.105	0.103	0.113	0.115	0	0	0	0	0	0	0	0	0
$\text{LaTi}_2\text{Al}_9\text{O}_{19}$	A_4	0.042	0.131	0.124	0.111	0.082	0.082	0.088	0	0	0	0	0	0	0	0	0
$\text{La}_2\text{Zr}_2\text{O}_7$	A_5	0.085	0.075	0.089	0.098	0.113	0.114	0.074	0	0	0	0	0	0	0	0	0
Mg_2SiO_4	A_6	0.254	0.055	0.063	0.113	0.106	0.116	0.190	0	0	0	0	0	0	0	0	0
$\text{La}_2\text{Hf}_2\text{O}_7$	A_7	0.142	0.059	0.069	0.100	0.091	0.113	0.154	0	0	0	0	0	0	0	0	0
$\text{La}_2\text{Ce}_2\text{O}_7$	A_8	0.095	0.147	0.169	0.133	0.216	0.071	0.074	0	0	0	0	0	0	0	0	0
$\text{Gd}_2\text{Zr}_2\text{O}_7$	A_9	0.092	0.169	0.165	0.117	0.079	0.192	0.102	0	0	0	0	0	0	0	0	0

Table 8. Limit matrix – thermal (50%) and mechanical (50%)

Properties		f_1	f_2	f_3	f_4	f_5	f_6	f_7	A_1	A_2	A_3	A_4	A_5	A_6	A_7	A_8	A_9
C_p	f_1	0.112	0.112	0.112	0.112	0.112	0.112	0.112	0	0	0	0	0	0	0	0	0
D_{th}	f_2	0.150	0.150	0.150	0.150	0.150	0.150	0.150	0	0	0	0	0	0	0	0	0
λ	f_3	0.122	0.122	0.122	0.122	0.122	0.122	0.122	0	0	0	0	0	0	0	0	0
α	f_4	0.116	0.116	0.116	0.116	0.116	0.116	0.116	0	0	0	0	0	0	0	0	0
E	f_5	0.140	0.140	0.140	0.140	0.140	0.140	0.140	0	0	0	0	0	0	0	0	0
H_V	f_6	0.156	0.156	0.156	0.156	0.156	0.156	0.156	0	0	0	0	0	0	0	0	0
K_{IC}	f_7	0.204	0.204	0.204	0.204	0.204	0.204	0.204	0	0	0	0	0	0	0	0	0
SrZrO_3	A_1	0	0	0	0	0	0	0	0.092	0.092	0.092	0.092	0.092	0.092	0.092	0.092	0.092
Yb_3NbO_7	A_2	0	0	0	0	0	0	0	0.113	0.113	0.113	0.113	0.113	0.113	0.113	0.113	0.113
Yb_3TaO_7	A_3	0	0	0	0	0	0	0	0.117	0.117	0.117	0.117	0.117	0.117	0.117	0.117	0.117
$\text{LaTi}_2\text{Al}_9\text{O}_{19}$	A_4	0	0	0	0	0	0	0	0.095	0.095	0.095	0.095	0.095	0.095	0.095	0.095	0.095
$\text{La}_2\text{Zr}_2\text{O}_7$	A_5	0	0	0	0	0	0	0	0.092	0.092	0.092	0.092	0.092	0.092	0.092	0.092	0.092
Mg_2SiO_4	A_6	0	0	0	0	0	0	0	0.129	0.129	0.129	0.129	0.129	0.129	0.129	0.129	0.129
$\text{La}_2\text{Hf}_2\text{O}_7$	A_7	0	0	0	0	0	0	0	0.106	0.106	0.106	0.106	0.106	0.106	0.106	0.106	0.106
$\text{La}_2\text{Ce}_2\text{O}_7$	A_8	0	0	0	0	0	0	0	0.125	0.125	0.125	0.125	0.125	0.125	0.125	0.125	0.125
$\text{Gd}_2\text{Zr}_2\text{O}_7$	A_9	0	0	0	0	0	0	0	0.131	0.131	0.131	0.131	0.131	0.131	0.131	0.131	0.131

Table 9. Limit matrix – thermal (60%) and mechanical (40%)

Properties		f_1	f_2	f_3	f_4	f_5	f_6	f_7	A_1	A_2	A_3	A_4	A_5	A_6	A_7	A_8	A_9
C_p	f_1	0.133	0.133	0.133	0.133	0.133	0.133	0.133	0	0	0	0	0	0	0	0	0
D_{th}	f_2	0.182	0.182	0.182	0.182	0.182	0.182	0.182	0	0	0	0	0	0	0	0	0
λ	f_3	0.147	0.147	0.147	0.147	0.147	0.147	0.147	0	0	0	0	0	0	0	0	0
α	f_4	0.138	0.138	0.138	0.138	0.138	0.138	0.138	0	0	0	0	0	0	0	0	0
E	f_5	0.112	0.112	0.112	0.112	0.112	0.112	0.112	0	0	0	0	0	0	0	0	0
H_V	f_6	0.125	0.125	0.125	0.125	0.125	0.125	0.125	0	0	0	0	0	0	0	0	0
K_{IC}	f_7	0.164	0.164	0.164	0.164	0.164	0.164	0.164	0	0	0	0	0	0	0	0	0
SrZrO_3	A_1	0	0	0	0	0	0	0	0.088	0.088	0.088	0.088	0.088	0.088	0.088	0.088	0.088
Yb_3NbO_7	A_2	0	0	0	0	0	0	0	0.117	0.117	0.117	0.117	0.117	0.117	0.117	0.117	0.117
Yb_3TaO_7	A_3	0	0	0	0	0	0	0	0.118	0.118	0.118	0.118	0.118	0.118	0.118	0.118	0.118

LaTi₂Al₉O₁₉	A₄	0	0	0	0	0	0	0	0.097	0.097	0.097	0.097	0.097	0.097	0.097	0.097	0.097
La₂Zr₂O₇	A₅	0	0	0	0	0	0	0	0.091	0.091	0.091	0.091	0.091	0.091	0.091	0.091	0.091
Mg₂SiO₄	A₆	0	0	0	0	0	0	0	0.126	0.126	0.126	0.126	0.126	0.126	0.126	0.126	0.126
La₂Hf₂O₇	A₇	0	0	0	0	0	0	0	0.103	0.103	0.103	0.103	0.103	0.103	0.103	0.103	0.103
La₂Ce₂O₇	A₈	0	0	0	0	0	0	0	0.128	0.128	0.128	0.128	0.128	0.128	0.128	0.128	0.128
Gd₂Zr₂O₇	A₉	0	0	0	0	0	0	0	0.133	0.133	0.133	0.133	0.133	0.133	0.133	0.133	0.133

Table 10. Limit matrix – thermal (70%) and mechanical (30%)

Properties		<i>f</i> ₁	<i>f</i> ₂	<i>f</i> ₃	<i>f</i> ₄	<i>f</i> ₅	<i>f</i> ₆	<i>f</i> ₇	<i>A</i> ₁	<i>A</i> ₂	<i>A</i> ₃	<i>A</i> ₄	<i>A</i> ₅	<i>A</i> ₆	<i>A</i> ₇	<i>A</i> ₈	<i>A</i> ₉
C_p	<i>f</i>₁	0.153	0.153	0.153	0.153	0.153	0.153	0.153	0	0	0	0	0	0	0	0	0
D_{th}	<i>f</i>₂	0.214	0.214	0.214	0.214	0.214	0.214	0.214	0	0	0	0	0	0	0	0	0
λ	<i>f</i>₃	0.173	0.173	0.173	0.173	0.173	0.173	0.173	0	0	0	0	0	0	0	0	0
α	<i>f</i>₄	0.160	0.160	0.160	0.160	0.160	0.160	0.160	0	0	0	0	0	0	0	0	0
E	<i>f</i>₅	0.084	0.084	0.084	0.084	0.084	0.084	0.084	0	0	0	0	0	0	0	0	0
H_v	<i>f</i>₆	0.093	0.093	0.093	0.093	0.093	0.093	0.093	0	0	0	0	0	0	0	0	0
K_{IC}	<i>f</i>₇	0.123	0.123	0.123	0.123	0.123	0.123	0.123	0	0	0	0	0	0	0	0	0
SrZrO₃	<i>A</i>₁	0	0	0	0	0	0	0	0.085	0.085	0.085	0.085	0.085	0.085	0.085	0.085	0.085
Yb₃NbO₇	<i>A</i>₂	0	0	0	0	0	0	0	0.120	0.120	0.120	0.120	0.120	0.120	0.120	0.120	0.120
Yb₃TaO₇	<i>A</i>₃	0	0	0	0	0	0	0	0.120	0.120	0.120	0.120	0.120	0.120	0.120	0.120	0.120
LaTi₂Al₉O₁₉	<i>A</i>₄	0	0	0	0	0	0	0	0.099	0.099	0.099	0.099	0.099	0.099	0.099	0.099	0.099
La₂Zr₂O₇	<i>A</i>₅	0	0	0	0	0	0	0	0.089	0.089	0.089	0.089	0.089	0.089	0.089	0.089	0.089
Mg₂SiO₄	<i>A</i>₆	0	0	0	0	0	0	0	0.123	0.123	0.123	0.123	0.123	0.123	0.123	0.123	0.123
La₂Hf₂O₇	<i>A</i>₇	0	0	0	0	0	0	0	0.099	0.099	0.099	0.099	0.099	0.099	0.099	0.099	0.099
La₂Ce₂O₇	<i>A</i>₈	0	0	0	0	0	0	0	0.130	0.130	0.130	0.130	0.130	0.130	0.130	0.130	0.130
Gd₂Zr₂O₇	<i>A</i>₉	0	0	0	0	0	0	0	0.134	0.134	0.134	0.134	0.134	0.134	0.134	0.134	0.134

Table 11. Limit matrix – thermal (80%) and mechanical (20%)

Properties		<i>f</i> ₁	<i>f</i> ₂	<i>f</i> ₃	<i>f</i> ₄	<i>f</i> ₅	<i>f</i> ₆	<i>f</i> ₇	<i>A</i> ₁	<i>A</i> ₂	<i>A</i> ₃	<i>A</i> ₄	<i>A</i> ₅	<i>A</i> ₆	<i>A</i> ₇	<i>A</i> ₈	<i>A</i> ₉
C_p	<i>f</i>₁	0.172	0.172	0.172	0.172	0.172	0.172	0.172	0	0	0	0	0	0	0	0	0
D_{th}	<i>f</i>₂	0.248	0.248	0.248	0.248	0.248	0.248	0.248	0	0	0	0	0	0	0	0	0
λ	<i>f</i>₃	0.199	0.199	0.199	0.199	0.199	0.199	0.199	0	0	0	0	0	0	0	0	0
α	<i>f</i>₄	0.181	0.181	0.181	0.181	0.181	0.181	0.181	0	0	0	0	0	0	0	0	0
E	<i>f</i>₅	0.056	0.056	0.056	0.056	0.056	0.056	0.056	0	0	0	0	0	0	0	0	0
H_v	<i>f</i>₆	0.062	0.062	0.062	0.062	0.062	0.062	0.062	0	0	0	0	0	0	0	0	0
K_{IC}	<i>f</i>₇	0.082	0.082	0.082	0.082	0.082	0.082	0.082	0	0	0	0	0	0	0	0	0
SrZrO₃	<i>A</i>₁	0	0	0	0	0	0	0	0.082	0.082	0.082	0.082	0.082	0.082	0.082	0.082	0.082
Yb₃NbO₇	<i>A</i>₂	0	0	0	0	0	0	0	0.124	0.124	0.124	0.124	0.124	0.124	0.124	0.124	0.124
Yb₃TaO₇	<i>A</i>₃	0	0	0	0	0	0	0	0.121	0.121	0.121	0.121	0.121	0.121	0.121	0.121	0.121
LaTi₂Al₉O₁₉	<i>A</i>₄	0	0	0	0	0	0	0	0.101	0.101	0.101	0.101	0.101	0.101	0.101	0.101	0.101
La₂Zr₂O₇	<i>A</i>₅	0	0	0	0	0	0	0	0.088	0.088	0.088	0.088	0.088	0.088	0.088	0.088	0.088
Mg₂SiO₄	<i>A</i>₆	0	0	0	0	0	0	0	0.119	0.119	0.119	0.119	0.119	0.119	0.119	0.119	0.119
La₂Hf₂O₇	<i>A</i>₇	0	0	0	0	0	0	0	0.095	0.095	0.095	0.095	0.095	0.095	0.095	0.095	0.095
La₂Ce₂O₇	<i>A</i>₈	0	0	0	0	0	0	0	0.133	0.133	0.133	0.133	0.133	0.133	0.133	0.133	0.133
Gd₂Zr₂O₇	<i>A</i>₉	0	0	0	0	0	0	0	0.136	0.136	0.136	0.136	0.136	0.136	0.136	0.136	0.136

Table 12. Final ranking of materials

Cluster weight (Thermal: Mechanical)	Results	SrZrO ₃	Yb ₃ NbO ₇	Yb ₃ TaO ₇	LaTi ₂ Al ₉ O ₁₉	La ₂ Zr ₂ O ₇	Mg ₂ SiO ₄	La ₂ Hf ₂ O ₇	La ₂ Ce ₂ O ₇	Gd ₂ Zr ₂ O ₇
50:50	Score	0,092	0,113	0,117	0,095	0,092	0,129	0,106	0,125	0,131
	Rank	9	5	4	7	8	2	6	3	1
60:40	Score	0.088	0.117	0.118	0.097	0.091	0.126	0.103	0.128	0.133
	Rank	9	5	4	7	8	3	6	2	1

70:30	Score	0.085	0.120	0.120	0.099	0.089	0.123	0.099	0.130	0.134
	Rank	9	4	5	7	8	3	6	2	1
80:20	Score	0.082	0.124	0.121	0.101	0.088	0.119	0.095	0.133	0.136
	Rank	9	3	4	6	8	5	7	2	1

2) $\text{La}_2\text{Ce}_2\text{O}_7$ takes second place (except 50:50 – third place) by a small margin, also in all sets of weights. $\text{La}_2\text{Ce}_2\text{O}_7$ can also be considered the second-best material.

3) Mg_2SiO_4 , Yb_3NbO_7 and Yb_3TaO_7 share 3rd, 4th and 5th places (except 50:50 where Mg_2SiO_4 takes second place) depending on the set of weights and can be considered as suitable materials.

4) $\text{La}_2\text{Hf}_2\text{O}_7$, $\text{LaTi}_2\text{Al}_9\text{O}_{19}$, $\text{La}_2\text{Zr}_2\text{O}_7$ and SrZrO_3 took the last places, and these materials can be considered less suitable or unsuitable.

4. Conclusion

This paper primarily focuses on determining the best oxide material for the TBC system using the ANP approach. The thermal and mechanical properties of the main oxide materials used for thermal barrier coatings have been presented. Having feedback allows us to get more information about how to fix the problem. ANP also provides a greater

degree of freedom to the decision maker, which makes it possible to divide criteria into clusters and assign appropriate weights (significance) to them. Two clusters (thermal and mechanical) with three weights were considered in this case.

Overall, based on the obtained results, the material $\text{Gd}_2\text{Zr}_2\text{O}_7$ was identified as the best candidate for the top layer of the TBC system.

Once the top coat material has been selected, its effectiveness in the TBC system is directly dependent on the composition of the other layer materials. Given that the TBC system consists of not one, but a complex of several materials (multilayer system), the performance of this system depends not only on the top coat oxide material (and its properties), but also on the properties of other materials in the composition and their combined use. Future investigations should focus on studying the use of this selected oxide material in combination with other materials in the system.

References

- [1] William W. Bathie, *Fundamentals of Gas Turbines*, 2nd Edition, Wiley: New York, NY, USA, 1996. [[Google Scholar](#)] [[Publisher Link](#)]
- [2] John H. Perepezko, “The Hotter the Engine, the Better,” *Science*, vol. 326, no. 5956, pp. 1068-1069, 2009. [[CrossRef](#)] [[Google Scholar](#)] [[Publisher Link](#)]
- [3] David R. Clarke, Matthias Oechsner, and Nitin P. Padture, “Thermal Barrier Coatings for More Efficient Gas-Turbine Engines,” *MRS Bulletin*, vol. 37, no. 10, pp. 891-898, 2012. [[CrossRef](#)] [[Google Scholar](#)] [[Publisher Link](#)]
- [4] David R. Clarke, and Simon R. Phillpot, “Thermal Barrier Coating Materials,” *Materials Today*, vol. 8, no. 6, pp. 22-29, 2005. [[CrossRef](#)] [[Google Scholar](#)] [[Publisher Link](#)]
- [5] Jeanine T. DeMasi-Marcin, and Dinesh K. Gupta, “Protective Coatings in the Gas-Turbine Engine,” *Surface and Coatings Technology*, vol. 68-69, pp. 1-9, 1994. [[CrossRef](#)] [[Google Scholar](#)] [[Publisher Link](#)]
- [6] A.G. Evans, D.R. Clarke, and C.G. Levi, “The Influence of Oxides on the Performance of Advanced Gas Turbines,” *Journal of the European Ceramic Society*, vol. 28, no. 7, pp. 1405-1419, 2008. [[CrossRef](#)] [[Google Scholar](#)] [[Publisher Link](#)]
- [7] A.G. Evans et al., “Mechanisms Controlling the Durability of Thermal Barrier Coatings,” *Progress in Materials Science*, vol. 46, no. 5, pp. 505-553, 2001. [[CrossRef](#)] [[Google Scholar](#)] [[Publisher Link](#)]
- [8] Brian Gleeson, “Thermal Barrier Coatings for Aeroengine Applications,” *Journal of Propulsion and Power*, vol. 22, no. 2, 2006. [[CrossRef](#)] [[Google Scholar](#)] [[Publisher Link](#)]
- [9] G.W. Goward, “Progress in Coatings for Gas Turbine Airfoils,” *Surface and Coatings Technology*, vol. 108-109, pp. 73-79, 1998. [[CrossRef](#)] [[Google Scholar](#)] [[Publisher Link](#)]
- [10] Carlos G. Levi, “Emerging Materials and Processes for Thermal Barrier Systems,” *Current Opinion in Solid State and Materials Science*, vol. 8, no. 1, pp. 77-91, 2004. [[CrossRef](#)] [[Google Scholar](#)] [[Publisher Link](#)]
- [11] Robert Vaßen et al., “Overview on Advanced Thermal Barrier Coatings,” *Surface and Coatings Technology*, vol. 205, no. 4, pp. 938-942, 2010. [[CrossRef](#)] [[Google Scholar](#)] [[Publisher Link](#)]
- [12] D.R. Clarke, and C.G. Levi, “Materials Design for the Next Generation Thermal Barrier Coatings,” *Annual Review of Materials Research*, vol. 33, pp. 383-417, 2003. [[CrossRef](#)] [[Google Scholar](#)] [[Publisher Link](#)]
- [13] Nitin P. Padture, Maurice Gell, and Eric H. Jordan, “Thermal Barrier Coatings for Gas-Turbine Engine Applications,” *Science*, vol. 296, no. 5566, pp. 280-284, 2002. [[CrossRef](#)] [[Google Scholar](#)] [[Publisher Link](#)]
- [14] William J. Brindley, and Robert A. Miller, “TBCs for Better Engine Efficiency,” *Advanced Materials and Processes*, vol. 136, 1989. [[Google Scholar](#)] [[Publisher Link](#)]

- [15] M. Peters et al., “EB-PVD Thermal Barrier Coating for Aeroengines and Gas Turbines,” *Advanced Engineering materials*, vol. 3, no. 4, pp. 193-204, 2001. [[CrossRef](#)] [[Google Scholar](#)] [[Publisher Link](#)]
- [16] D.V. Rigney et al., “PVD Thermal Barrier Coating Applications and Process Development for Aircraft Engines,” *Journal of Thermal Spray Technology*, vol. 6, pp. 167-175, 1997. [[CrossRef](#)] [[Google Scholar](#)] [[Publisher Link](#)]
- [17] Bertrand Saint-Ramond, “HITS - High Insulation Thermal Barrier Coating Systems,” *Air and Space Europe*, vol. 3, no. 3-4, pp. 174-177, 2001. [[CrossRef](#)] [[Google Scholar](#)] [[Publisher Link](#)]
- [18] X.Q. Cao, R. Vassen, and D. Stoeber, “Ceramic Materials for Thermal Barrier Coatings,” *Journal of the European Ceramic Society*, vol. 24, no. 1, pp. 1-10, 2004. [[CrossRef](#)] [[Google Scholar](#)] [[Publisher Link](#)]
- [19] Jinbao Song et al., “Multi-Scale Structural Design and Advanced Materials for Thermal Barrier Coatings with High Thermal Insulation: A Review,” *Coatings*, vol. 13, no. 2, 2023. [[CrossRef](#)] [[Google Scholar](#)] [[Publisher Link](#)]
- [20] A.S. Milani et al., “An Application of the Analytic Network Process in Multiple Criteria Material Selection,” *Materials and Design*, vol. 44, pp. 622-632, 2013. [[CrossRef](#)] [[Google Scholar](#)] [[Publisher Link](#)]
- [21] Thomas L. Saaty, *Decision Making with Dependence and Feedback: The Analytic Network Process*, RWS Publications, Pittsburgh, USA, 1996. [[Google Scholar](#)] [[Publisher Link](#)]
- [22] Wen Ma et al., “Perovskite-Type Strontium Zirconate as a New Material for Thermal Barrier Coatings,” *Journal of the American Ceramic Society*, vol. 91, no. 8, pp. 2630-2635, 2008. [[CrossRef](#)] [[Google Scholar](#)] [[Publisher Link](#)]
- [23] W. Ma et al., “Yb₂O₃ and Gd₂O₃ Doped Strontium Zirconate for Thermal Barrier Coatings,” *Journal of the European Ceramic Society*, vol. 28, no. 16, pp. 3071-3081, 2008. [[CrossRef](#)] [[Google Scholar](#)] [[Publisher Link](#)]
- [24] Lin Chen, et al., “Thermo-Mechanical Properties of Fluorite Yb₃TaO₇ and Yb₃NbO₇ Ceramics with Glass-like Thermal Conductivity,” *Journal of Alloys and Compounds*, vol. 788, pp. 1231-1239, 2019. [[CrossRef](#)] [[Google Scholar](#)] [[Publisher Link](#)]
- [25] Xiaoyun Xie et al., “Lanthanum-Titanium-Aluminum Oxide: A Novel Thermal Barrier Coating Material for Applications at 1300°C,” *Journal of the European Ceramic Society*, vol. 31, no. 9, pp. 1677-1683, 2011. [[CrossRef](#)] [[Google Scholar](#)] [[Publisher Link](#)]
- [26] Robert Vassen et al., “Zirconates as New Materials for Thermal Barrier Coatings,” *Journal of the American Ceramic Society*, vol. 83, no. 8, pp. 2023-2028, 2000. [[CrossRef](#)] [[Google Scholar](#)] [[Publisher Link](#)]
- [27] D. Stöver et al., “New Material Concepts for the Next Generation of Plasma-Sprayed Thermal Barrier Coatings,” *Journal of Thermal Spray Technology*, vol. 13, pp. 76-83, 2004. [[CrossRef](#)] [[Google Scholar](#)] [[Publisher Link](#)]
- [28] Henry Lehmann et al., “Thermal Conductivity and Thermal Expansion Coefficients of the Lanthanum Rare-Earth-Element Zirconate System,” *Journal of the American Ceramic Society*, vol. 86, no. 8, pp. 1338-1344, 2003. [[CrossRef](#)] [[Google Scholar](#)] [[Publisher Link](#)]
- [29] Si Chen et al., “Mg₂SiO₄ as a Novel Thermal Barrier Coating Material for Gas Turbine Applications,” *Journal of the European Ceramic Society*, vol. 39, no. 7, pp. 2397-2408, 2019. [[CrossRef](#)] [[Google Scholar](#)] [[Publisher Link](#)]
- [30] Panpan Liang et al., “La₂Hf₂O₇ Ceramics as Potential Top-Coat Materials for Thermal/Environmental Barrier Coatings,” *Ceramics International*, vol. 45, no. 17, 22432-22436, 2019. [[CrossRef](#)] [[Google Scholar](#)] [[Publisher Link](#)]
- [31] Jian-Wei Dai et al., “Effects of ZrO₂ Doping on Mechanical and Thermo-Physical Properties of La₂Ce₂O₇ Ceramics,” *Equipment Environmental Engineering*, vol. 16, no. 10, pp. 21-26, 2019. [[Publisher Link](#)]
- [32] Ying Liu et al., “Preparation and Characterization of SrZrO₃-La₂Ce₂O₇ Composite Ceramics as a Thermal Barrier Coating Material,” *Materials Chemistry and Physics*, vol. 247, 2020. [[CrossRef](#)] [[Google Scholar](#)] [[Publisher Link](#)]
- [33] W. Ma et al., “Synthesis and Thermophysical Properties of Gd₂Zr₂O₇/SrZrO₃ Composite as a Thermal Barrier Coating Material,” *Thermal Spray Proceedings*, pp. 56-61, 2016. [[CrossRef](#)] [[Google Scholar](#)] [[Publisher Link](#)]